06

Formation of ordered perovskite nanostructures by nanoimprinting

© D.V. Lebedev[1–3], F.M. Kochetkov[1,3], A.A. Yakubova[1], N.A. Solomonov[1,3], R. Kenesbay[1], D.V. Minev[1], S.V. Makarov[4], I.S. Mukhin[1,3]

[1] Alferov Federal State Budgetary Institution of Higher Education and Science Saint Petersburg National Research Academic University of the Russian Academy of Sciences, St. Petersburg, Russia
[2] Institute of Analytical Instrument Making, Russian Academy of Sciences, St. Petersburg, Russia
[3] Peter the Great Saint-Petersburg Polytechnic University, St. Petersburg, Russia
[4] ITMO University, St. Petersburg, Russia
E-mail: Denis.v.lebedev@gmail.com

Received November 5, 2025
Revised November 21, 2025
Accepted November 24, 2025

A new versatile method for synthesis of ordered nanostructures from halide perovskite $CsPbBr_3$ by nanoimprinting is proposed and implemented experimentally. The method allows one to form extensive (with an area up to 25 mm^2) homogeneous regions containing two types of perovskite structures: ordered arrays of individual nanoparticles and microflakes with a nanostructured surface. A study of the optical properties of the synthesized samples by photoluminescence microspectroscopy revealed narrow resonance emission peaks at 523 nm for a particle array and at 525 nm for flakes (the width of the spectral line at half maximum was 19 and 21 nm, respectively). The intensity of photoluminescence, which is determined by the total volume of excited perovskite material, was significantly higher in the case of flakes.

Keywords: nanostructures, perovskites, optical spectroscopy, synthesis technique.

DOI: 10.61011/TPL.2026.03.63068.20558

The use of materials with unique optical and electronic properties opens up new opportunities for development and examination of passive and active photonic components. This class of materials includes halide perovskites, which have been studied extensively in the last decade [1]. Perovskite materials have many applications in optoelectronics, including light-emitting diodes [2,3], solar cells [4], lasers [5], photodetectors [6], etc. This is largely attributable to their unique properties: relatively high mobility of carriers, long mean free path, high absorption and photoluminescence quantum yield, and the potential to adjust the band gap over a wide range by varying the composition [7–14]. Note also that perovskites have a narrow spectral emission line and a wider color gamut than organic molecules and inorganic quantum dots [15].

The synthesis of nanostructured and nanopatterned perovskite materials (ordered arrays of nanocrystals included) is a key requirement for control over their optoelectronic properties [16,17]. This architecture helps minimize losses due to carrier scattering and recombination and increase the efficiency of radiation outcoupling from the active region, which is crucial for fabrication of highly efficient and stable next-generation devices, such as light-emitting diodes (PeLEDs), lasers, and photodetectors. Several approaches to synthesis of ordered (patterned) arrays of perovskite nanocrystals are known [18]. Top-down methods, such as electron beam lithography, provide high positioning accuracy, but are expensive and hard to implement, and the material may be damaged in the process (among other things, through chemical action of the resist and developers themselves). Note that current methods for patterning of perovskites (e.g., electron beam lithography) often cause degradation of their optical properties due to chemical and radiation damage. Bottom-up approaches based on porous matrices do not provide the required positioning accuracy and control over morphology. Bottom-up approaches involving the use of porous templates (e.g., anodic alumina) and controlled crystallization methods, which allow for direct formation of dense and homogeneous arrays through self-assembly and controlled nucleation in specified regions, are more widespread. These include the nanoimprinting technique [19,20], which has got into general use due to a number of advantages: high resolution and homogeneity, processing rate and low cost, and relatively mild synthesis conditions.

In the present study, we propose a new method for synthesis of ordered nanostructured arrays of perovskite materials. The results for $CsPbBr_3$, which is stable under atmospheric conditions [21], are presented. Nanoimprinting, which relies on physical pressing (impression) to form a nanoscale relief, is used for this purpose.

The diagram of the sample synthesis process is presented in Fig. 1. At the first stage, a patterned polymer matrix is formed. Its relief serves as a negative for subsequent structuring of the perovskite. A commercially available GaN/sapphire structured wafer (GLO AB NanoLund), which is an array of hexagonally periodic gallium nitride nanotrapezoids, was used as a master template to produce this negative. The period of the nanotrapezoid array was 1 μm. The template was placed on the bottom of a Petri

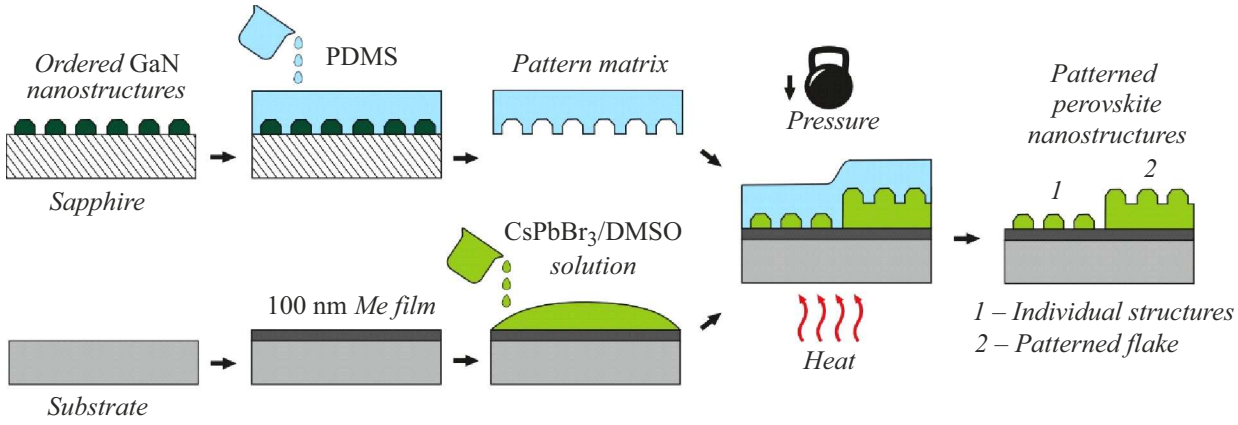

Figure 1. Schematic diagram of the procedure of synthesis of patterned perovskite arrays.

dish, and liquid polydimethylsiloxane (PDMS) precursor was then poured onto it. Curing in a drying oven at a temperature of 80 °C was performed for 30 min to the point of complete polymerization of the elastomer. PDMS was chosen as the master template material for forming perovskite nanostructure arrays for a number of reasons, such as its high elasticity, the ease of synthesis of micro- and nanostructures, and compatibility with soft nanoimprinting. The Young's modulus of PDMS ranges from 0.5 to 3 MPa [22], while the Young's modulus of perovskite $CsPbBr_3$ is measured at 17–26 GPa [23]. This difference in values allows one to use PDMS as a template without risking the damage or deformation of perovskite structures. The resulting master template was separated from the substrate with a scalpel and stored in a desiccator under a slight excess nitrogen pressure. These storage conditions are needed to minimize contamination of the master template. Note that the templates obtained this way are reusable for at least 50 times.

Growth substrates were prepared at the next stage. Various types of surfaces, including cover glass, sapphire, and silicon wafers (both uncoated and with metallized layers of Ni, Pt, etc.), were used in the study. All the tested substrates were found to be suitable for synthesis of patterned perovskite, confirming the wide applicability of the method to dielectric and metallized surfaces. The synthesis on a platinum film deposited by thermal evaporation onto a low-resistance silicon wafer is considered below. This substrate was chosen for its applicability in electro-optical measurements, since it provides direct formation of an electrical contact to the perovskite layer. The typical size of the obtained sample was 10×10 mm. Before use, the growth substrate surface was processed in an ultrasonic bath in deionized water, acetone, and isopropanol (10 min with each liquid in sequence). The sample was then dried on a hotplate at 150 °C for 10 min. At the final stage of preparation, the substrate surface was activated in oxygen plasma (40 W, 10 min, 0.3 mbar). Next, 5 μl of fresh 0.2 M solution of $CsPbBr_3$ salts in dimethyl sulfoxide were applied to the substrate surface. The $CsPbBr_3$ solution was prepared in an inert nitrogen atmosphere by dissolving $PbBr_2$ (99.9 % pure, Lankhit) and CsBr (99.9 % pure, Lankhit) with a molar concentration of 0.2 mM/ml in anhydrous 99.8 % dimethyl sulfoxide (Sigma Aldrich) with subsequent stirring at 300 rpm for 12 h at a temperature of 60 °C. At the final stage of perovskite synthesis, the prepared master template and the substrate with the precursor were compressed mechanically (Fig. 1) and heated to 60 °C for 2 h. With the heat treatment completed, the template was separated from the surface on which ordered arrays of $CsPbBr_3$ nanostructures were formed.

The surface morphology and topography of the synthesized samples were investigated with a Zeiss Supra 25 scanning electron microscope (SEM) and an Ntegra (NT-MDT) atomic force microscope (AFM). CSG01 probes (NT-MDT) were used for AFM measurements.

Figure 2 shows typical SEM and AFM images illustrating the formation of two types of $CsPbBr_3$ nanostructures. The first type is ordered individual nanoparticles that were synthesized in the cavities of the master template and follow its hexagonal periodicity (1 μm). They are $\sim$ 400 nm in diameter and $\sim$ 250 nm in height. The size of these individual nanoparticles deviates by no more than 10 % from the average value. Pronounced faceting may be indicative of their high crystallinity. The samples of the second type are flakes with a lateral size of 1–50 μm and a thickness up to 1 μm. Their surface also has a periodic pattern (with a period of $\sim$ 1 μm), but with a more developed relief, where the height of individual elements relative to a flake reaches a level of $\sim$ 500 nm. Note also that the diameter of a single element on a flake is $\sim$ 1000 nm. Apparently, extended flakes form due to growth surface–template gapping and to an excess of precursor solution. Note that the proposed technique allows one to synthesize homogeneous nanostructured perovskite coatings up to 5×5 mm in size.

The optical properties of the synthesized samples were studied using photoluminescence (PL) spectroscopy. PL spectra of all the mentioned types of perovskite samples were recorded at an excitation wavelength of 365 nm (I-line

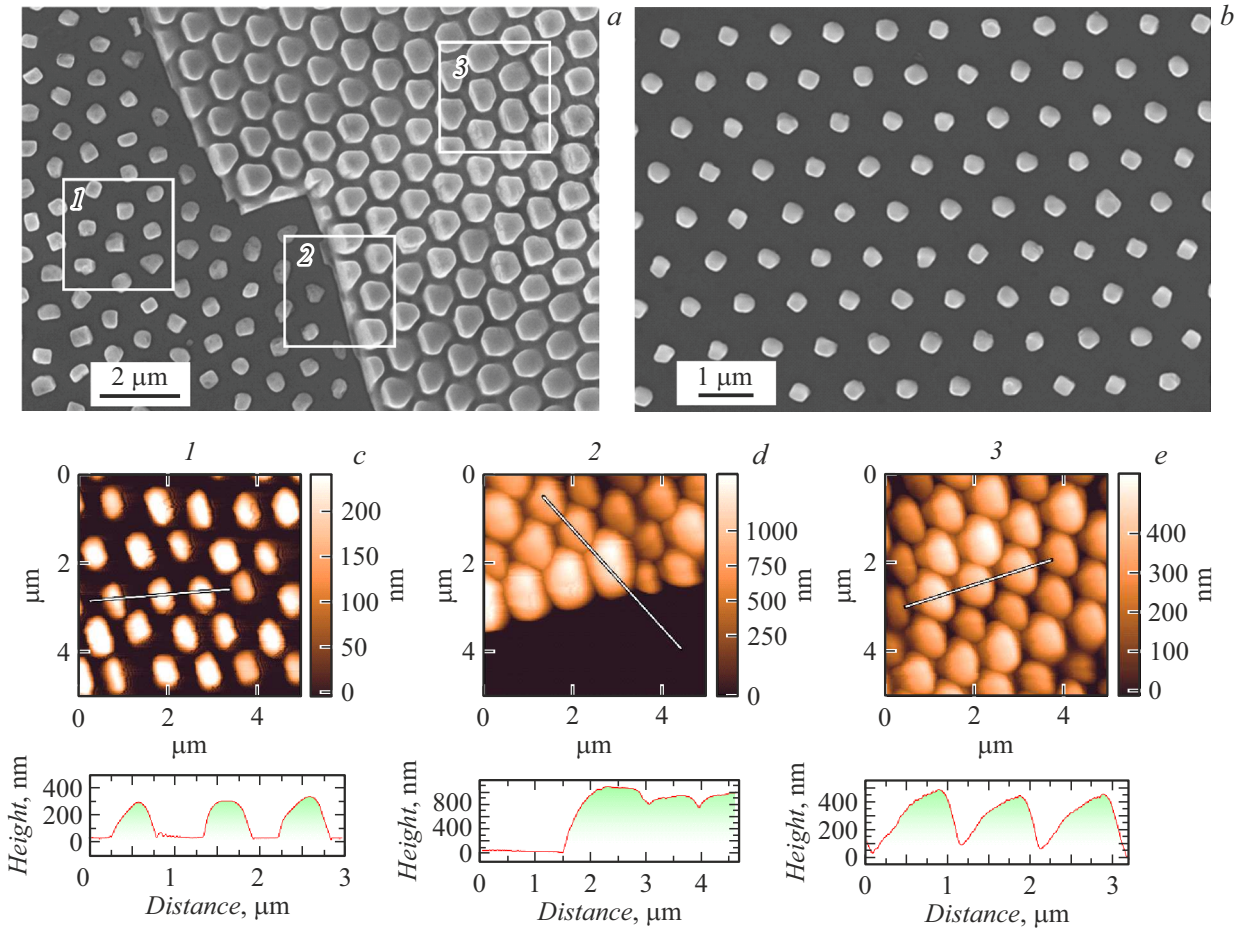

Figure 2. Morphological studies of the obtained samples. *a* — SEM image of the substrate surface with formed patterned $CsPbBr_3$ nanostructures (nanoparticles and a flake); *b* — section of the sample surface with an ordered array of $CsPbBr_3$ nanoparticles; *c*–*e* — AFM surface topography of different regions highlighted by squares and numbered in panel *a* and the corresponding surface profiles.

of a mercury UV lamp). Fluorescence images of the samples were obtained using an Axio Imager A2m (Carl Zeiss) microscope with 100 × EC Epiplan-NEOFLUAR (Carl Zeiss) objectives. PL spectra were recorded by a QE Pro (Ocean Optics) fiber optic spectrometer coupled to the specified microscope in the fluorescence mode. The diameter of the detection region (radiation collection region) was $2\,\mu$m. Figure 3 shows the PL spectra recorded in regions containing an array of individual $CsPbBr_3$ nanoparticles and a single flake. Clear PL peaks are seen both for the array and the flake at 523 and at 525 nm (with a FWHM of 19 and 21 nm, respectively). The intensity of PL from the flake is several times higher than that of the array of nanoparticles. This is attributable to the difference in volume of excited perovskite (both nanoparticles and the flake contribute to the PL signal).

The efficiency of soft nanoimprinting in synthesis of ordered arrays of $CsPbBr_3$ nanostructures was demonstrated in the present study. The key advantage of the proposed approach is its simplicity and versatility, which is crucial for integration into optoelectronic devices. Note that the results of spectroscopy and morphology studies reveal that the structure remains stable for at least three months under atmospheric conditions.

It was found that two types of morphologically different structures are formed in the process of synthesis.

1. Ordered arrays of individual nanoparticles. The obtained array of perovskite particles is a fine model for the study of collective effects, such as super- and hyperluminescence and the formation of polariton states in a periodic system, and for the fabrication of nanolasers with a low pumping threshold. Ordering is crucial for control over the radiation modes in this case.

2. Microflakes with their own periodic nanostructure. These objects are a hybrid of a bulk crystal and a photonic crystal. The periodic relief on their surface may act as a diffraction grating or a photonic crystal, effectively outcoupling radiation from the active medium. Thus, these structures hold promise for application in light-emitting diodes (PeLEDs) with increased light extraction efficiency.

Despite the morphological differences, both types of structures feature high crystallinity and characteristic narrow PL peaks in the green region of the spectrum (523–525 nm). The emission of flakes is more intense.

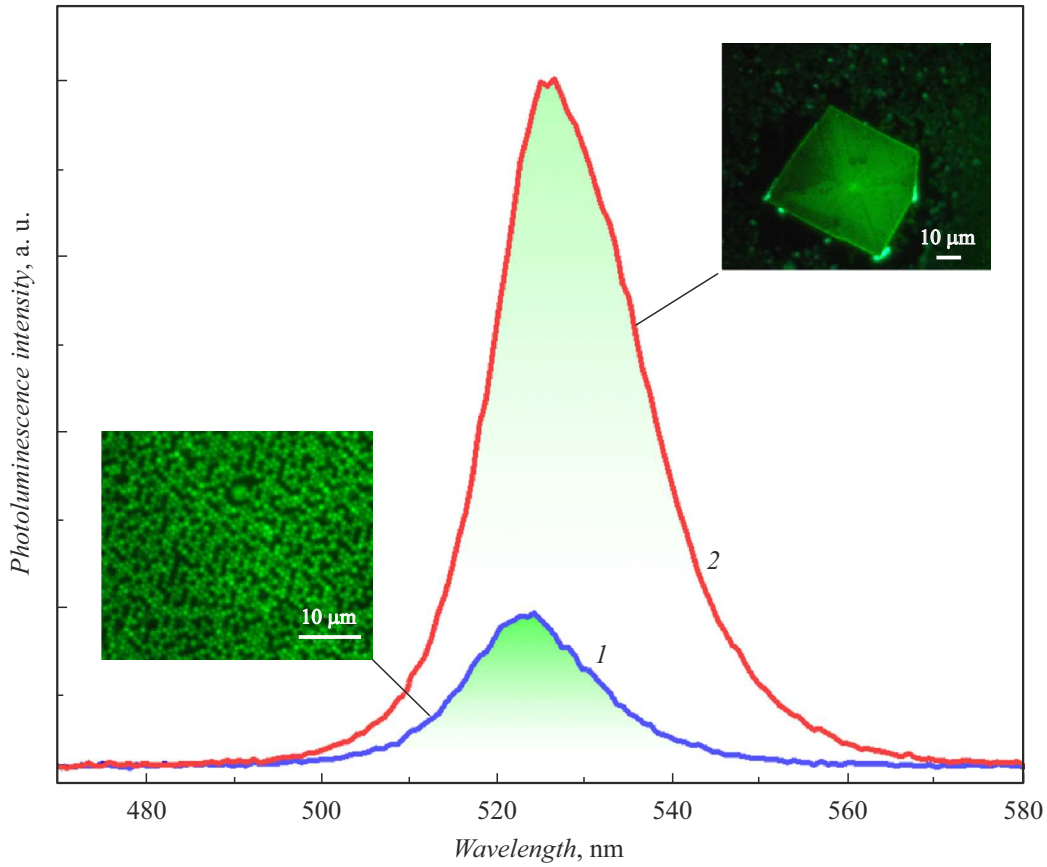

Figure 3. Photoluminescence spectra of two types of obtained $CsPbBr_3$ samples: *1* — array of individual nanoparticles; *2* — flake. Optical microscope images of the samples illuminated with ultraviolet radiation with a wavelength of 365 nm are shown in the insets. Color highlighting under the curves was done to increase the contrast.

Thus, a reproducible, scalable, and cost-effective method of synthesis of ordered arrays of halide perovskite nanoparticles was developed. It enables controlled fabrication of high-quality patterned layers for nanophotonic and optoelectronic applications.

Funding

This study was supported financially by the Russian Science Foundation (project No. 25-19-00666).

Conflict of interest

The authors declare that they have no conflict of interest.

References

[1] P. Docampo, T. Bein, Acc. Chem. Res., **49**, 339 (2016). DOI: 10.1021/acs.accounts.5b00465
[2] M. Lu, J. Guo, P. Lu, L. Zhang, Y. Zhang, Q. Dai, Y. Hu, V.L. Colvin, W.W. Yu, J. Phys. Chem. C, **123**, 22787 (2019). DOI: 10.1021/acs.jpcc.9b06144
[3] A. Fakharuddin, M.K. Gangishetty, M. Abdi-Jalebi, S.-H. Chin, A.R. bin Mohd Yusoff, D.N. Congreve, W. Tress, F. Deschler, M. Vasilopoulou, H.J. Bolink, Nat. Electron., **5**, 203 (2022). DOI: 10.1038/s41928-022-00745-7
[4] A.R. bin Mohd Yusoff, M.K. Nazeeruddin, Adv. Energy Mater., **8**, 1702073 (2018). DOI: 10.1002/aenm.201702073
[5] Y. Shi, X. Deng, Y. Gan, L. Xu, Q. Zhang, Q. Xiong, Adv. Mater., **37**, e2413559 (2025). DOI: 10.1002/adma.202413559
[6] M. Ahmadi, T. Wu, B. Hu, Adv. Mater., **29**, 1605242 (2017). DOI: 10.1002/adma.201605242
[7] S.D. Stranks, G.E. Eperon, G. Grancini, C. Menelaou, M.J.P. Alcocer, T. Leijtens, L.M. Herz, A. Petrozza, H.J. Snaith, Science, **342**, 341 (2013). DOI: 10.1126/science.1243982
[8] Q. Dong, Y. Fang, Y. Shao, P. Mulligan, J. Qiu, L. Cao, J. Huang, Science, **347**, 967 (2015). DOI: 10.1126/science.aaa5760
[9] G. Xing, N. Mathews, S. Sun, S.S. Lim, Y.M. Lam, M. Grätzel, S. Mhaisalkar, T.C. Sum, Science, **342**, 344 (2013). DOI: 10.1126/science.1243167
[10] S. Wieghold, J. Tresback, J.-P. Correa-Baena, N.T.P. Hartono, S. Sun, Z. Liu, M. Layurova, Z.A. VanOrman, A.S. Bieber, J. Thapa, B. Lai, Z. Cai, L. Nienhaus, T. Buonassisi, Chem. Mater., **31**, 3712 (2019). DOI: 10.1021/acs.chemmater.9b00650
[11] J.-P. Correa-Baena, Y. Luo, T.M. Brenner, J. Snaider, S. Sun, X. Li, M.A. Jensen, N.T.P. Hartono, L. Nienhaus, S. Wieghold, J.R. Poindexter, S. Wang, Y.S. Meng, T. Wang, B. Lai, M.V. Holt, Z. Cai, M.G. Bawendi, L. Huang, T. Buonassisi, D.P. Fenning, Science, **363**, 627 (2019). DOI: 10.1126/science.aah5065

[12] S.S. Shin, J.P. Correa-Baena, R.C. Kurchin, A. Polizzotti, J.J. Yoo, S. Wieghold, M.G. Bawendi, T. Buonassisi, Chem. Mater., **30**, 336 (2018). DOI: 10.1021/acs.chemmater.7b03227
[13] S. Wieghold, J.-P. Correa-Baena, L. Nienhaus, S. Sun, K.E. Shulenberger, Z. Liu, J.S. Tresback, S.S. Shin, M.G. Bawendi, T. Buonassisi, ACS Appl. Energy Mater., **1**, 6801 (2018). DOI: 10.1021/acsaem.8b00913
[14] J.-P. Correa-Baena, L. Nienhaus, R.C. Kurchin, S.S. Shin, S. Wieghold, N.T. Putri Hartono, M. Layurova, N.D. Klein, J.R. Poindexter, A. Polizzotti, S. Sun, M.G. Bawendi, T. Buonassisi, Chem. Mater., **30**, 3734 (2018). DOI: 10.1021/acs.chemmater.8b00676
[15] J. Zhang, C. Wang, X. Shen, M. Lu, J. Guo, X. Bai, Y. Zhang, W.W. Yu, Appl. Phys. Lett., **115**, 193104 (2019). DOI: 10.1063/1.5120848
[16] J.S. Du, D. Shin, T.K. Stanev, C. Musumeci, Z. Xie, Z. Huang, M. Lai, L. Sun, W. Zhou, N.P. Stern, V.P. Dravid, C.A. Mirkin, Sci. Adv., **6**, eabc4959 (2020). DOI: 10.1126/sciadv.abc4959
[17] J. Shamsi, A.S. Urban, M. Imran, L. De Trizio, L. Manna, Chem. Rev., **119**, 3296 (2019). DOI: 10.1021/acs.chemrev.8b00644
[18] J.W. Han, S.H. Hwang, M.J. Seol, S.Y. Kim, Adv. Opt. Mater., **10**, 2200534 (2022). DOI: 10.1002/adom.202200534
[19] N. Pourdavoud, S. Wang, A. Mayer, T. Hu, Y. Chen, A. Marianovich, W. Kowalsky, R. Heiderhoff, H. Scheer, T. Riedl, Adv. Mater., **29**, 1605003 (2017). DOI: 10.1002/adma.201605003
[20] Y. Shen, L.-P. Cheng, Y.-Q. Li, W. Li, J.-D. Chen, S.-T. Lee, J.-X. Tang, Adv. Mater., **31**, 1901517 (2019). DOI: 10.1002/adma.201901517
[21] N. Kumar, J. Rani, R. Kurchania, Solar Energy, **221**, 197 (2021). DOI: 10.1016/j.solener.2021.04.042
[22] A. Mata, A.J. Fleischman, S. Roy, Biomed. Microdevices, **7**, 281 (2005). DOI: 10.1007/s10544-005-6070-2
[23] M. Aktary, M. Kamruzzaman, R. Afrose, RSC Adv., **12**, 23704 (2022). DOI: 10.1039/D2RA04591E

Translated by D.Safin